Applied Surface Science 308 (2014) 58–62

Contents lists available at ScienceDirect

Applied Surface Science

journal homepage: www.elsevier.com/locate/apsusc

Electrode patterning of ITO thin films by high repetition rate fiber laser

H.K. Lin*, W.C. Hsu

Graduate Institute of Materials Engineering, National Pingtung University of Science and Technology, Pingtung 912, Taiwan, ROC

ARTICLE INFO

Article history:
Received 5 November 2013
Received in revised form 20 March 2014
Accepted 12 April 2014
Available online 28 April 2014

Keywords:
Indium tin oxide (ITO)
Laser annealing
Wet etching

ABSTRACT

Indium tin oxide (ITO) thin films are deposited on glass substrates using a radio frequency magnetron sputtering system. As-deposited ITO thin film was 100 nm in thickness and a transmittance of ITO film on glass substrate was 79% at 550 nm. Conductive electrodes are then patterned on the ITO films using a high repetition rate fiber laser system followed by a wet chemical etching process. The electrical, optical and structural properties of the patterned samples are evaluated by means of a four-point probe technique, spectrophotometer, X-ray diffraction (XRD), scanning electron microscopy (SEM) and atomic force microscopy (AFM). The results show that the samples annealed with a pulse repetition rate of 150 kHz or 400 kHz have a low sheet resistivity of 21 Ω/□ and a high optical transmittance of 90%. In addition, it is shown that a higher pulse repetition rate reduces both the residual stress and the surface roughness of the patterned specimens. Therefore, the present results suggest that a pulse repetition rate of 400 kHz represents the optimal processing condition for the patterning of crack-free ITO-coated glass substrates with good electrical and optical properties.

1. Introduction

Transparent conductive oxides (TCOs) deposited on glass or plastic substrates have a light weight, good flexibility and a high optical transmittance [1]. Among the various TCOs available, indium tin oxide (ITO) has many favorable properties, including a low electrical resistance ($\sim 1.5 \times 10^{-4}$ ohm cm), a good adhesion ability on glass, a high optical transparency, a good resistance to acidic environments, and a high electrical and chemical stability. As a result, it has been used for a wide variety of applications, including flat panel displays, organic light-emitting diodes (OLEDs), cholesteric liquid crystal displays, and solar cells [2–6].

ITO electrodes are generally patterned using traditional photolithography techniques followed by annealing in a hot furnace [7]. However, such an approach is not only complex and time-consuming, but may also result in substrate damage due to the high temperatures involved in the annealing process (i.e., ~200 °C). Accordingly, the use of laser ablation to pattern ITO electrodes directly has attracted increasing attention in recent decades [8–17]. Broadly speaking, existing laser patterning methods utilize either long-pulses (nanoseconds) [8–10,14–16] or ultrafast-pulses (picoseconds or femtoseconds) [11–13]. Yavas [8,9] showed that ITO films deposited on lime glass or fused quartz substrates was patterned using different wavelength lasers. It is showed that the ablated quality of ITO films depends on both the underlying substrate material and the wavelength of the laser ablation system. Excimer (KrF, 248 nm) and DPSS lasers (355 and 1064 nm) with nanosecond pulse duration have been used for material patterning [10,18]. Meanwhile, it was shown that when patterning ITO substrates using a nanosecond pulse duration, a laser wavelength of 355 nm results in well-defined grooves, whereas a higher wavelength of 1064 nm leads to a significant accumulation of ablated material at the groove edges.

In general, direct laser ablation provides a quick, versatile and low-cost solution for patterning ITO thin films. However, a high laser energy is required to heat the ITO material to a sufficient temperature to cause melting and evaporation. As a result, the substrate is easily damaged dues to thermally induced stresses. Especially for devices that are fabricated directly onto the substrate and easily led to material accumulation onto edge of the ablation trench, meaning that this approach has a number of limitations. Accordingly, the use of a combined laser annealing and wet etching process to pattern ITO thin films has attracted increasing attention in recent years [19,20]. In such an approach, the ITO film is patterned using a low irradiation energy; with the aim being simply to prompt a transformation of the original amorphous ITO phase to a crystalline phase (leading to a corresponding change in the subsequent etching rate) rather than to melt and remove the ITO material directly. However, in adopting direct laser ablation methods, the pulse repetition rate must be carefully controlled since an excessive input energy (i.e.,

---

* Corresponding author. Tel.: +886 8 7703202 7568.
E-mail address: HKLin@mail.npust.edu.tw (H.K. Lin).

http://dx.doi.org/10.1016/j.apsusc.2014.04.084
0169-4332/© 2014 Elsevier B.V. All rights reserved.

a longer laser pulse) results in a cracking of the ITO films and subsequent electrical failure [19,21]. It was shown that for ITO films deposited on glass substrates and then etched in oxalic acid, the optical and electrical properties are enhanced when patterning is performed using a high repetition rate femtosecond laser [20].

The present study proposes a technique for fabricating crack-free ITO-coated patterned substrates using a fiber laser and a wet etching process. The patterning process is performed using pulse repetition rates ranging from 100 to 400 kHz. The optimal repetition rate is determined by evaluating the electrical, optical and structural properties of the various samples using a four-point probe technique, spectrophotometer, X-ray diffraction (XRD), scanning electron microscopy (SEM) and atomic force microscopy (AFM).

2. Experimental

ITO thin films with a thickness of approximately 100 nm were deposited on glass substrates (AGC G2, thickness: 0.7 mm) under ambient temperature conditions using a RF magnetron sputtering system (UNI-4500, Japan) with an In_2O_3 (90 wt.%):SnO_2 (10 wt.%) target (Well Being). The deposition process was performed using a working power of 3 kW; a sputtering time of 29 s; and Ar, H_2 and O_2 flow rates of 22, 5 and 6 sccm, respectively. The ITO samples were then annealed using a fiber laser (SPI-12, UK) with a wavelength of 1064 nm and repetition rates ranging from 100 to 400 kHz. In every case, the irradiation power was set as 470 mW, the scanning speed was set to 5 mm/s, a spot size of 42 μm, a pulse duration of 30 ns, and the scanning pitch was set as 25 μm. Following the ablation process, the specimens were immersed in 0.05 M oxalic acid etchant at 40 °C for 4 min.In the annealing process, the pulse energy (E) is given by [22]

$$E = \frac{P_{\mathrm{AVG}}}{\mathrm{rep}}, \tag{1}$$

where P_{AVG} and rep denote the average power of a pulse laser and laser repetition rates, respectively. From Eq. (1), it is seen that the pulse energy reduces as the repetition rate increases. For the laser system used in the present study, the pulse energy had values of 4.7, 3.8. 3.1 and 1.2 μJ for the considered repetition rates of 100, 125, 150 and 400 kHz, respectively. The electrical and optical properties of the various specimens were investigated before and after wet etching using a four-point probe technique (SR-H1000C, Taiwan) and a UV–vis spectrophotometer (Lambda 35, USA), respectively. Meanwhile, the crystalline properties of the ITO samples were examined using an X-ray diffraction method (XRD, Bruker D8 Advance, Germany) with a Cu-Kα radiation source and a scanning range of 20–80°. The surface morphologies were examined using a field emission scanning electron microscope (FESEM, JSM-7600F, Japan). The surface roughness of the films was measured using an atomic force microscope (AFM, Veeco di CP-II) and the measured area is 10 μm × 10 μm. Finally, the residual stress of the ITO thin films was measured using a grazing incidence X-ray diffraction (GIXRD) system based on the conventional $\sin^2\Psi$ method [23].

3. Results and discussion

Fig. 1 shows the sheet resistance of the various ITO thin-film samples before and after chemical etching. It is seen that the as-deposited ITO thin film has a sheet resistance of 81 Ω/□ prior to chemical etching. However, the sheet resistance overflows following the etching process. For the sample patterned with a repetition rate of 100 kHz (i.e., a pulse laser energy of 4.7 μJ), the resistance overflows both before and after the etching process. Given a pulse repetition rate of 125 kHz, the sheet resistance of the annealed specimen reduces to 21 Ω/□ due to the enhanced mobility and reduced scattering of the carriers [7,24]. However, following the etching process, the sheet resistance increases to around 180 Ω/□. It is observed that the ITO samples patterned with a pulse repetition rate of 150 kHz or 400 kHz have a very low sheet resistance (∼21 Ω/□) in both the etched condition and the un-etched condition. In other words, it appears that a pulse laser energy of 3.1 μJ represents the critical value below which a low sheet resistance is obtained.

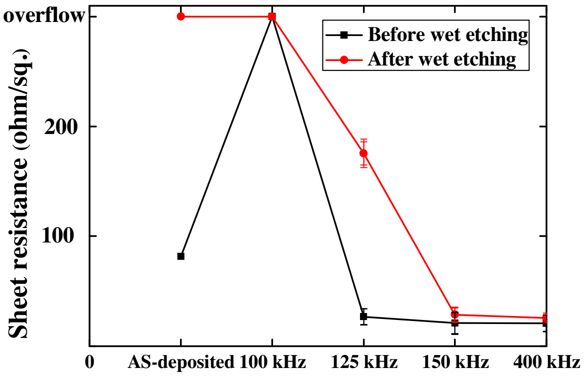

Fig. 1. Sheet resistance of as-deposited and annealed ITO samples before and after chemical etching.

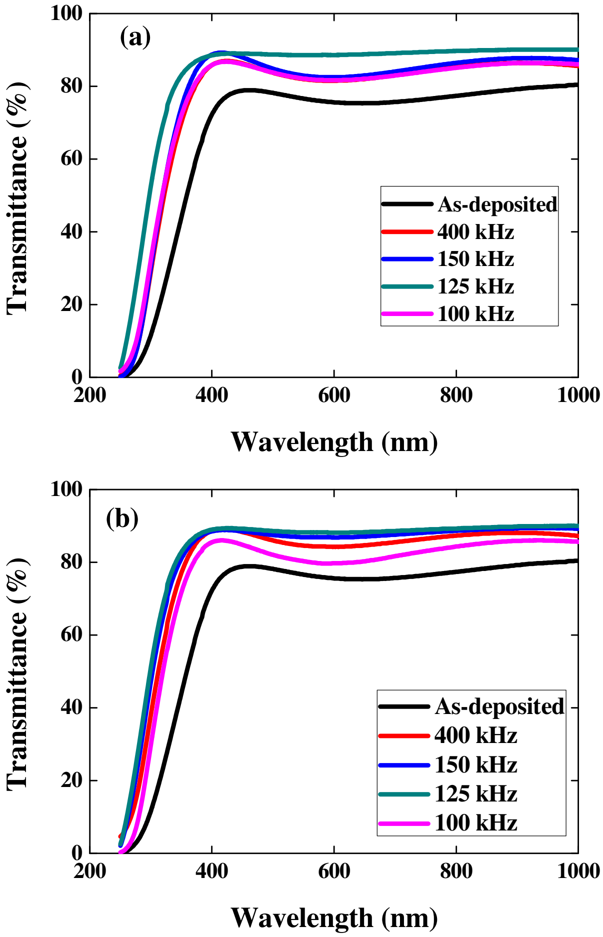

Fig. 2. Optical transmittance spectra of as-deposited and annealed ITO on glass samples (a) before and (b) after chemical etching.

Fig. 2(a) and (b) presents the optical transmittance spectra of the as-deposited and annealed ITO specimens before and after wet

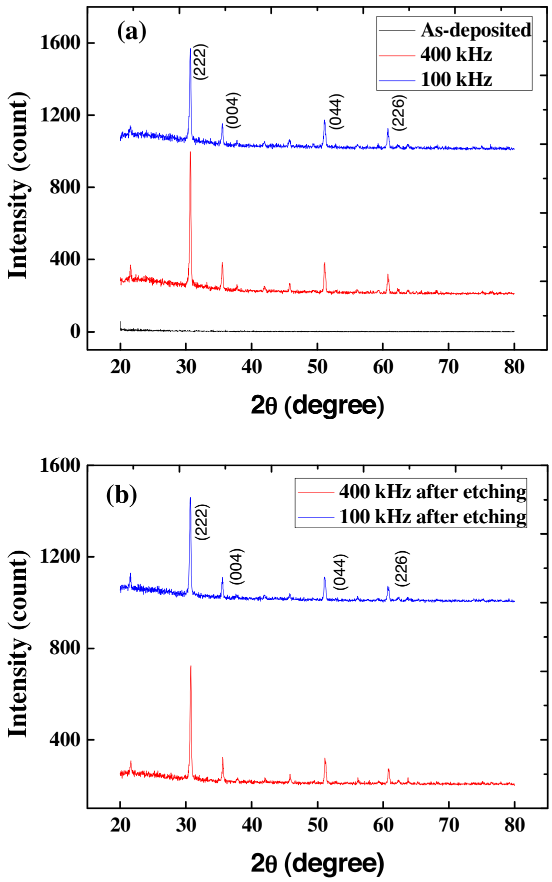

Fig. 3. XRD results for annealed ITO samples (a) before and (b) after chemical etching.

etching, respectively. It can be seen that all of the ITO films (both etched and un-etched) have good optical transparency in the visible range. From inspection, it is found that the annealing and etching process improves the transmittance from around 75% (as-deposited sample) to 90% given incident light with a wavelength of 550 nm. Fig. 3(a) presents the XRD spectra of the as-deposited ITO sample and un-etched ITO samples patterned with repetition rates of 100 kHz and 400 kHz, respectively. It is seen that the spectrum of the as-deposited sample contains no prominent peaks and it is amorphous structure. However, for the annealed samples, strong peaks corresponding to the (2 2 2), (0 4 4), (0 0 4) and (2 2 6) crystalline planes of indium tin oxide are observed. In other words, the annealing process prompts a change in the microstructure of the as-deposited ITO thin film from an amorphous state to a polycrystalline state. Fig. 3(b) confirms that the samples retain a polycrystalline structure following chemical etching. This observation is consistent with the general thermal annealing results [21].

Fig. 4 presents SEM images of the un-etched ITO samples patterned using laser pulse repetition rates of 100, 125, 150 and 400 kHz. It is observed that the sample annealed using a pulse repetition rate of 100 kHz contains a thick micro-crack. As discussed in Ref. [21], the micro-crack results from a difference in the residual stress between the irradiated and non-irradiated regions of the ITO thin film. Comparing the four SEM images, it is seen that the grain size reduces with an increasing pulse repetition rate (i.e., reducing pulse laser energy). Moreover, it is noted that the micro-cracking tendency of the annealed samples also reduces as the pulse repetition rate increases. Fig. 5 shows the surface morphologies of the annealed ITO thin films following the wet etching process. It is seen that the samples annealed with a pulse repetition rate of 150 kHz or 400 kHz retain a small and uniform grain size. However, the samples patterned with a low repetition rate of 100 kHz or 125 kHz both contain large micro-cracks. This result is consistent with the findings of Ref. [21] that the greater energy input associated with a lower pulse repetition rate prompts the formation of defects in the annealed ITO thin film, which subsequently serve as preferred sites for a higher etching rate during the wet chemical etching process and lead to the formation of micro-cracks as a result. Notably, the micro-cracks account for the resistance overflow observed in the corresponding samples in Fig. 1.

Fig. 6 shows the surface roughness values of the as-deposited ITO thin film and the ITO films patterned using pulse repetition rates of 100 kHz and 400 kHz, respectively. It is seen that the

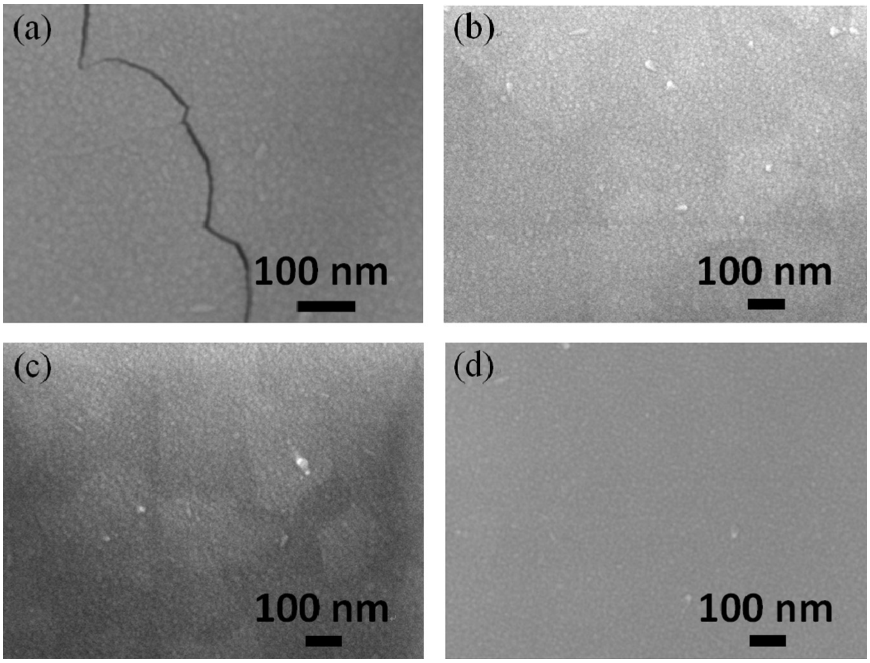

Fig. 4. SEM images of non-etched ITO samples annealed with repetition rates of: (a) 100 kHz, (b) 125 kHz, (c) 150 kHz and (d) 400 kHz.

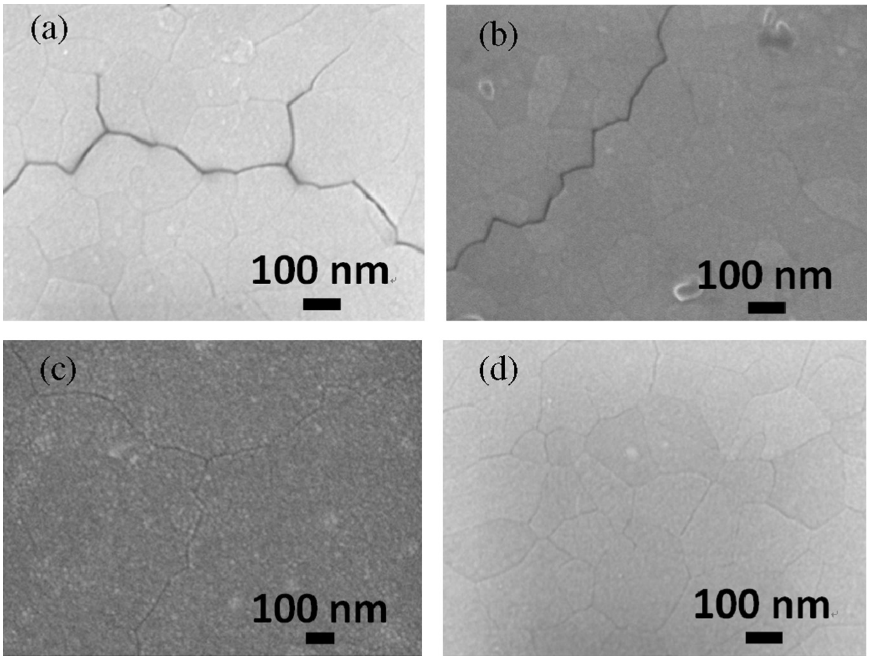

Fig. 5. SEM images of etched ITO samples annealed with repetition rates of: (a) 100 kHz, (b) 125 kHz, (c) 150 kHz and (d) 400 kHz.

as-deposited sample has a mean surface roughness of approximately 5 nm. For the annealed samples, the surface roughness reduces from 12.3 nm to 1.8 nm as the pulse repetition rate is increased from 100 kHz to 400 kHz. Moreover, the surface roughness of the two samples reduces to 4.6 nm and 1.5 nm, respectively, following the etching process. In other words, the effectiveness of a higher pulse repetition rate and a wet chemical etching process in reducing the surface roughness of the patterned ITO thin films is confirmed.

The residual stress in the etched laser-annealed ITO samples was measured using a GIXRD technique and was then compared with that of an ITO sample annealed at 200 °C for 1 hr in a furnace. For each of the three samples, Fig. 7 plots the variation of $(d - d_o)/d_o$ as a function of $\cos^2\alpha\sin^2\Psi$. Note that fixing the constant α angle, $\alpha = \theta_o - \gamma$, and tilting the different Ψ angle can get the variation where d_o is the initial lattice space (∼0.152 nm), using diffraction peaks 60.7°, incident angle 1°. Applying a linear regression technique to the experimental data, the gradients of the fitted slopes for the specimens annealed using pulse repetition rates of 100 kHz and 400 kHz were found to be 0.00373 and 0.00347, respectively, while that of the specimen annealed in the furnace has a value of 0.00106. For each specimen, the residual stress can be calculated using the slope equaling function $((1 + \nu)/E)\sigma$, where ν and E are the Poisson ratio (∼0.33) and Young's modulus (∼160 GPa) of ITO, respectively. Therefore, the residual stresses of the three specimens were found to be 448, 417 and 127 MPa, respectively. In other words, the residual stress reduces with a higher pulse repetition rate and the lower residual stress reduces the risk of cracking following the etching process, as observed in Fig. 5.

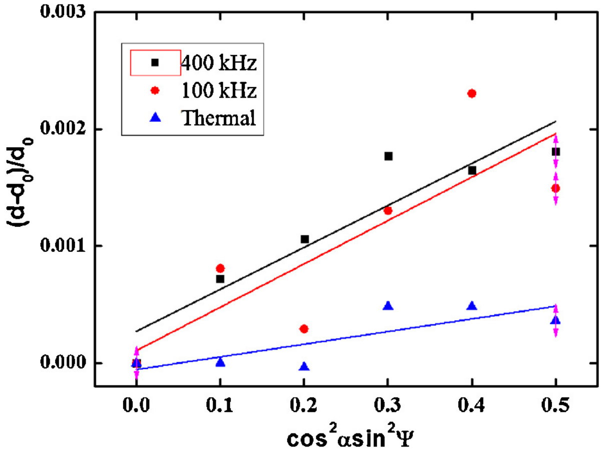

Fig. 7. The $(d - d_o)/d_o$ vs. $\cos^2\alpha\sin^2\Psi$ plot for traditional furnace-annealed ITO sample and ITO samples patterned using pulse repetition rates of 100 kHz and 400 kHz.

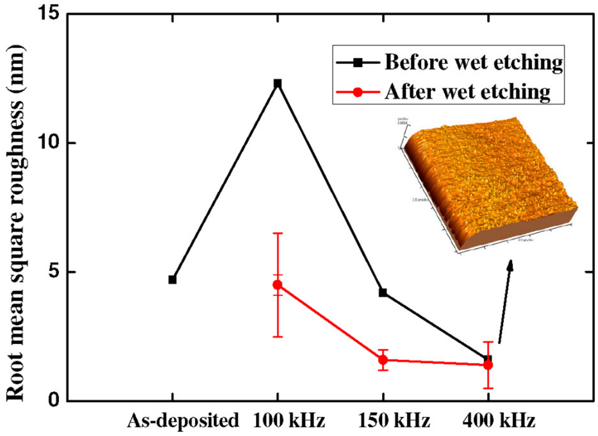

Fig. 6. Surface roughness of various etched and non-etched ITO samples. Note that inset shows AFM image of non-etched ITO sample patterned using pulse repetition rate of 400 kHz.

4. Conclusions

ITO thin films have been deposited on glass substrates and then patterned to form conductive electrodes using a laser annealing process followed by wet chemical etching. The laser patterning process has been performed using a fiber laser with a wavelength of 1064 nm and pulse repetition rates of 100, 125, 150 and 400 kHz, corresponding to laser pulse energies of 4.7, 3.8. 3.1 and 1.2 μJ, respectively. The results have shown that at lower pulse repetition rates (100 and 125 kHz), micro-cracks are formed in the etched samples; resulting in an overflow of the sheet resistance. However, as the pulse repetition rate is increased, the residual stress within the etched samples reduces, and thus the propensity for micro-cracking is reduced. Overall, the results have shown that a pulse repetition rate of 400 kHz results in a minimal sheet resistance, a high optical transmittance, a low surface roughness and a low residual stress, and is therefore the optimal annealing frequency for the ITO/glass samples.

Acknowledgements

The authors gratefully acknowledge the financial support provided to this study by the National Science Council of Taiwan, ROC under Project No. NSC102-2221-E-020-009. In addition, the authors wish to thank C.H. Li and B.C. Kung of ITRI for their useful input to the discussions during the course of the study.

References

[1] P.K. Biswas, A. De, L.K. Dua, L. Chkoda, Appl. Surf. Sci. 253 (2006) 1953–1959.
[2] U. Betz, M. Kharrazi Olsson, J. Marthy, M.F. Escolá, F. Atamny, Surf. Coat. Technol. 200 (2006) 5751–5759.
[3] C. Guillén, J. Herrero, Solar Energy Mater. Solar Cells 92 (2008) 938–941.
[4] A. Kloppel, B. Meyer, J. Trube, Thin Solid Films 392 (2001) 311–314.
[5] H. Kim, C.M. Gilmore, A. Piqué′, J.S. Horwitz, H. Mattoussi, H. Murata, Z.H. Kafafi, D.B. Chrisey, J. Appl. Phys. 86 (1999) 6451–6461.
[6] H.K. Lin, C.H. Li, S.H. Liu, Opt. Lasers Eng. 48 (2010) 1008–1011.
[7] H. Morikawa, M. Fujita, Thin Solid Films 359 (2000) 61–67.
[8] O. Yavas, C. Ochiai, M. Takai, Appl. Phys. A 69 (1999) S875–S878.
[9] O. Yavas, M. Takai, Appl. Phys. Lett. 73 (1998) 2558–2560.
[10] C. Molpeceres, S. Lauzurica, J.L. Ocaña, J.J. Gandía, L. Urbina, J. Cárabe, J. Micromech. Microeng. 15 (2005) 1271–1278.
[11] M. Park, B.H. Chon, H.S. Kim, S.C. Jeoung, D. Kim, J.-I. Lee, H.Y. Chu, H.R. Kim, Opt. Lasers Eng. 44 (2006) 138–146.
[12] H.W. Choi, D.F. Farson, J. Bovatsek, A. Arai, D. Ashkenasi, Appl. Opt. 46 (2007) 5792–5799.
[13] G. Račiukaitis, M. Brikas, M. Gedvilas, G. Darčianovas, JLMN – J. Laser Micro/Nanoeng. 2 (2007) 1–6.
[14] G. Legeay, X. Castel, R. Benzerga, J. Pinel, Phys. Stat. Solidi (C) 5 (2008) 3248–3254.
[15] Z.H. Li, E.S. Cho, S.J. Kwon, Appl. Surf. Sci. 255 (2009) 9843–9846.
[16] M.-F. Chen, W.-T. Hsiao, Y.-S. Ho, S.-F. Tseng, Y.-P. Chen, Thin Solid Films 518 (2009) 1072–1078.
[17] W.-T. Hsiao, S.-F. Tseng, K.-C. Huang, D. Chiang, Opt. Lasers Eng. 51 (2013) 15–22.
[18] J. Chae, L. Jang, K. Jain, Mater. Lett. 64 (2010) 948–950.
[19] C.-W. Cheng, J.-S. Chen, H.-H. Chen, Mater. Manuf. Processes 25 (2010) 684–688.
[20] C.-W. Cheng, C.-Y.i. Lin, W.-C. Shen, Y.-J. Lee, J.-S. Chen, Thin Solid Films 518 (2010) 7138–7142.
[21] C.J. Lee, H.K. Lin, C.H. Li, L.X. Chen, C.C. Lee, C.W. Wu, J.C. Huang, Thin Solid Films 522 (2012) 330–335.
[22] B.R. Benware, C.D. Macchietto, C.H. Moreno, J.J. Rocca, Phys. Rev. Lett. 81 (1998) 5804–5807.
[23] C.-H. Ma, J.-H. Huang, H. Chen, Thin Solid Films 418 (2002) 73–78.
[24] T.J. Coutts, D.L. Young, X. Li, MRS Bull. 25 (2000) 58–65.